Simplified Brushless Wound Field Synchronous Machine Topology Based on a Three-Phase Rectifier

SYED SABIR HUSSAIN BUKHARI[1,2], (Member, IEEE), **HAMZA AHMAD**[2], (Graduate Student Member, IEEE), **GHULAM JAWAD SIREWAL**[3], AND **JONG-SUK RO**[2]

[1]Department of Electrical Engineering, Sukkur IBA University, Sukkur 65200, Pakistan
[2]School of Electrical and Electronics Engineering, Chung-Ang University, Seoul 06974, South Korea
[3]Department of Electrical Engineering Technology, The Benazir Bhutto Shaheed University of Technology and Skill Development, Khairpur Mir's 66020, Pakistan

Corresponding author: Jong-Suk Ro (jongsukro@gmail.com)

ABSTRACT This paper proposes a novel simplified brushless wound field synchronous machine (BL–WFSM) topology based on an uncontrolled three-phase rectifier. The output of the rectifier is injected into the common point of the star-connected three-phase armature winding. This arrangement develops an armature MMF consisting of two components: the fundamental MMF, which is rotating in nature, and the harmonic pulsating magnetic field, which induces the harmonic current in the specially designed harmonic winding of the rotor. The induced harmonic current is rectified through the full-bridge rectifier, which excites the main rotor field to achieve brushless operation and produce torque while interacting with the main fundamental rotating field of the armature. The proposed brushless topology is simple as it involves a single three-phase rectifier which does not require any complicated control strategy. Furthermore, this topology is a cost-effective solution as compared to the conventional brushless WFSM topologies since it does not require any additional hardware component except for a typical rectifier. In addition, the performance of the proposed brushless topology is better than the existing three-phase rectifier-based brushless scheme in terms of efficiency, output torque, and torque ripple. The proposed simplified BL-WFSM topology is validated through 2-D finite element analysis (FEA) using JMAG-Designer 19.1 to obtain the output torque of the machine.

INDEX TERMS Brushless, cost-effective operation, harmonic field excitation, WRSMs.

I. INTRODUCTION

Permanent magnet (PM) machines except for those using ferrite magnets are not a preferred choice for the electrical machine manufacturing industry, especially when considering the low-power density applications [1]. The cost of rare-earth materials has recently hit new highs [2], [3]. This motivated researchers to explore other options that require no magnets. One of such candidates is a wound field synchronous machine (WFSM) [4], [5]. However, this machine requires brushes, slip rings, and additional exciters, which make them unfavorable for small- and medium-scale power applications [6], [7]. This encouraged researchers to work on

different brushless topologies of WFSMs based on harmonic field excitation techniques.

A brushless topology for WFSM based on zero-sequence third-harmonic field excitation was proposed in [8]. As shown in Fig. 1(a), this topology involves thyristor switches attached in between the inverter and the armature winding of the machine, which operates at zero-crossing of each phase current. This arrangement results in a zero-sequence third-harmonic current which generates a harmonic magnetic field in the airgap to induce harmonic current in the harmonic winding of the rotor to achieve brushless operation. The implementation of this brushless topology requires a complex control strategy and thyristor switches, which make it bulky and costly.

In [9], the authors proposed a brushless topology that required an extra winding to be installed in the stator

The associate editor coordinating the review of this manuscript and approving it for publication was Chi-Seng Lam.

(a)

(b)

(c)
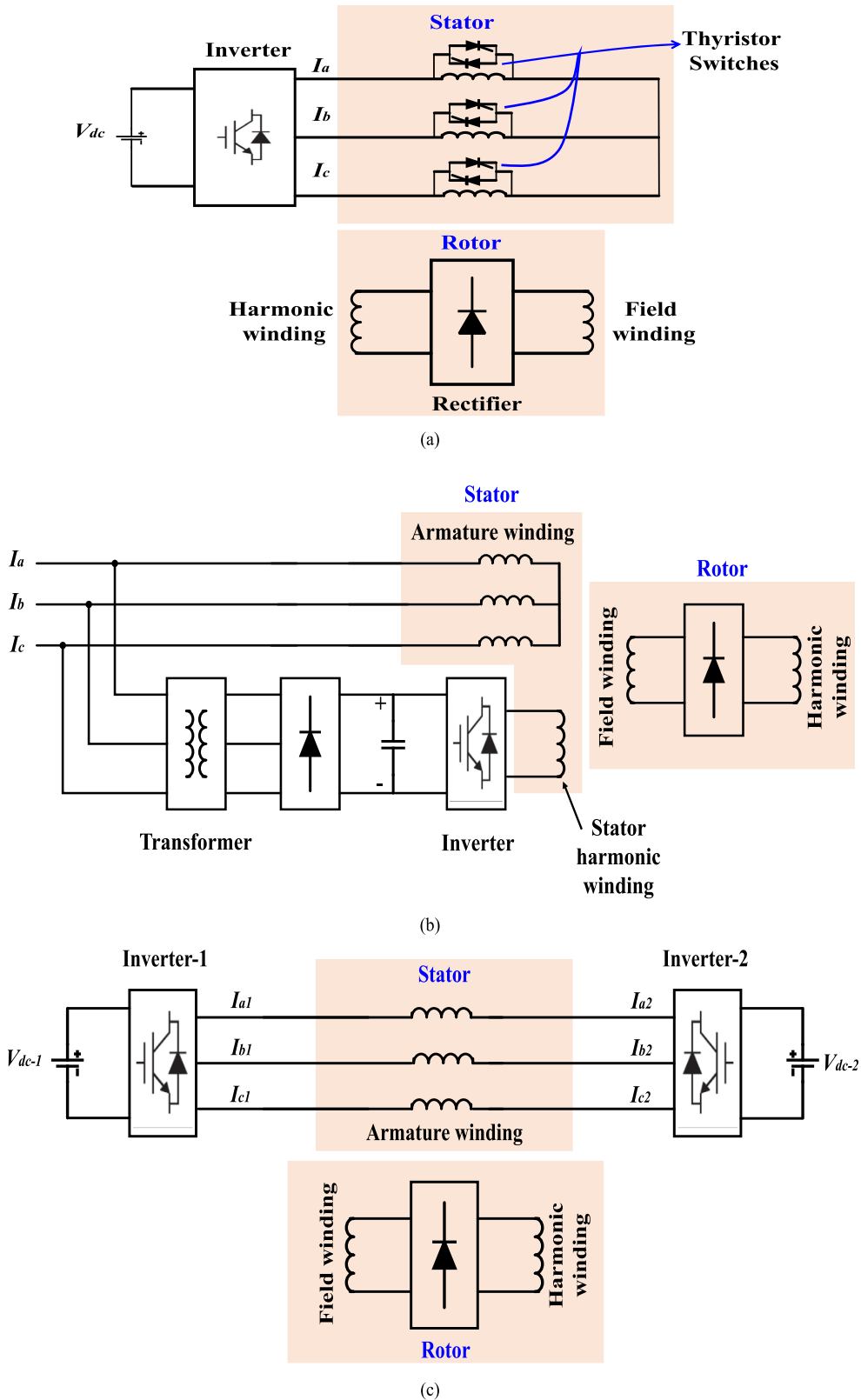
FIGURE 1. BL-WFSM topologies proposed in (a) [9]; (b) [10]; (c) [11–12].

slots in addition to the main armature winding, to inject a third-harmonic current and develop a third-harmonic MMF

in the airgap of the machine. As shown in Fig. 1(b), this topology requires a modification in the machine structure

(d)
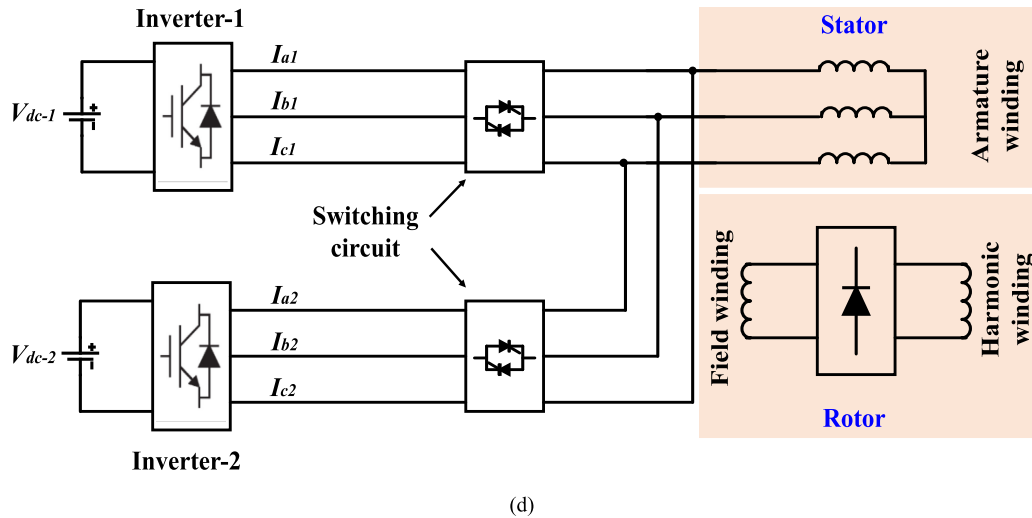
FIGURE 1. *(Continued.)* BL-WFSM topologies proposed in (d) [13].

and additional devices such as transformers and single-phase double-conversion converters, which may not be a preferable option for brushless operations in industrial applications.

In [10]–[12], the authors proposed brushless topologies based on dual-inverter-based configurations. In [10], [11], open-winding-pattern-based dual-inverter-fed brushless topologies were proposed to generate an armature current comprising fundamental and third-harmonic current components. In these topologies, the fundamental current is used to develop main field and the third-harmonic current is used to generate pulsating harmonic magnetic field in the airgap. The latter is used to induce harmonic current in the harmonic winding of the rotor to achieve brushless operation. The basic structure of these topologies is shown in Fig. 1(c). In [13], the same armature current was obtained by alternately operating two inverters. These inverters were attached in parallel as shown in Fig. 1(d) and were phase-shifted by −180° through thyristor switches, by turning them on and off after the completion of each cycle. The adoption of two inverters in these brushless topologies makes them costly and bulky.

In [14], a simpler BL-WFSM scheme was proposed to resolve the aforementioned issues. As shown in Fig. 2(a), the stator of the machine contains two windings i.e., three-phase main armature winding and a single two-pole exciter winding. These windings were connected through an uncontrolled rectifier. As the current flows through the armature winding, it is rectified through the rectifier to excite the exciter winding of the stator simultaneously. This arrangement generates two magnetic fields in the airgap, a four-pole magnetic field rotating at synchronous speed caused by the main armature current and a two-pole sub-harmonic pulsating magnetic field generated through the exciter winding current. The illustration of these magnetic fields is shown in Fig. 2(b). On the other hand, the rotor of the employed machine model is equipped with harmonic and field windings as shown in Fig. 2(c). The two-pole pulsating magnetic field induces a

harmonic current in the harmonic winding of the rotor which is then rectified to excite the main field winding to generate torque and achieve brushless operation. This topology offers several advantages over conventional BL-WFSM topologies such as simple machine structure, reduced drive size, low cost, reduced volume, and minimum control complications. Besides several advantages, some disadvantages associated with this topology are low average torque, high torque ripple, and low efficiency.

This paper proposes a simplified brushless WFSM topology by employing an uncontrolled customary three-phase rectifier that injects the output current to the common point of the star-connected three-phase armature winding. This arrangement generates a harmonic MMF in addition to the main armature MMF in the air gap of the machine. This harmonic MMF in turn generates the harmonic current in the harmonic winding of the machine, which is rectified to inject DC current to the rotor field winding through a full-bridge rectifier placed in between the harmonic and field windings. The interaction of the rotor and main rotating armature fields produces torque. The proposed simplified BL-WFSM topology is validated through 2-D finite element analysis (FEA) and its performance is compared with the existing three-phase rectifier-based BL-WFSM topology in terms of average output torque, torque ripple and efficiency. In addition, unlike the existing three-phase rectifier-based topology, the proposed topology does not require any additional winding to be installed with the main armature winding in the stator slots of the machine, which makes it even simpler compared to the existing topology.

II. OPERATING PRINCIPLE

The proposed simplified BL-WFSM topology and the employed 4-pole, 24-slot machine model are shown in Figs. 3(a) and (b), respectively. The stator and rotor winding configurations are presented in Fig. 4. The three-phase stator winding is star-connected with 100 number

(a)

(b)

(c)
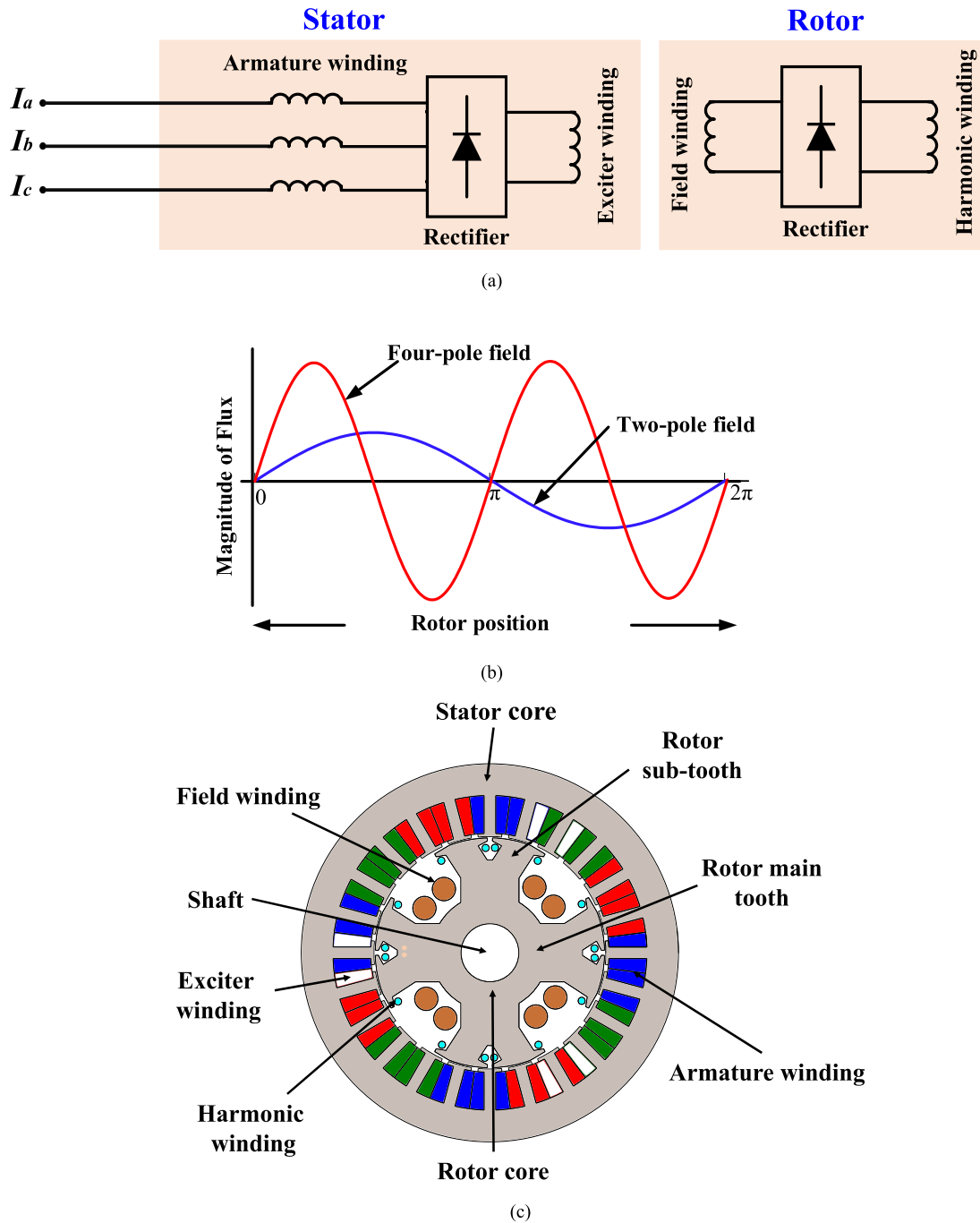
FIGURE 2. (a) Existing three-phase rectifier-based BL-WFSM topology, (b) airgap magnetic fields illustration, and (c) 2-D layout of the machine.

of turns per phase. The harmonic and field windings are connected through a full-bridge diode rectifier. The harmonic winding is installed on the each of the rotor sub-teeth and is having 25 number of turns. However, the field winding is wound around each of the rotor main teeth. The number of turns for the field winding of the machine are 250. The armature winding of the machine is supplied with a balanced three-phase current, as shown in Fig. 5(a). An uncontrolled customary three-phase rectifier whose one terminal is grounded, whereas the second terminal is attached to the common point of the star-connected armature winding of the machine is employed. The rectifier is supplied with I_{ar}, I_{br} and I_{cr} currents. The output of the rectifier (I_R) is shown in Fig. 5(b). This gives rise to the composite armature current as shown in Fig. 5(c). Fig. 6(a) shows the sum of the armature currents which indicates that unlike a balanced three-phase supply, the sum of the armature currents for the proposed BL-WFSM is not zero. Furthermore, the magnitude of the sum of the three-phase armature currents is the same as the output of the rectifier, that is, 0.82 A. This indicates that a

(a)

(b)
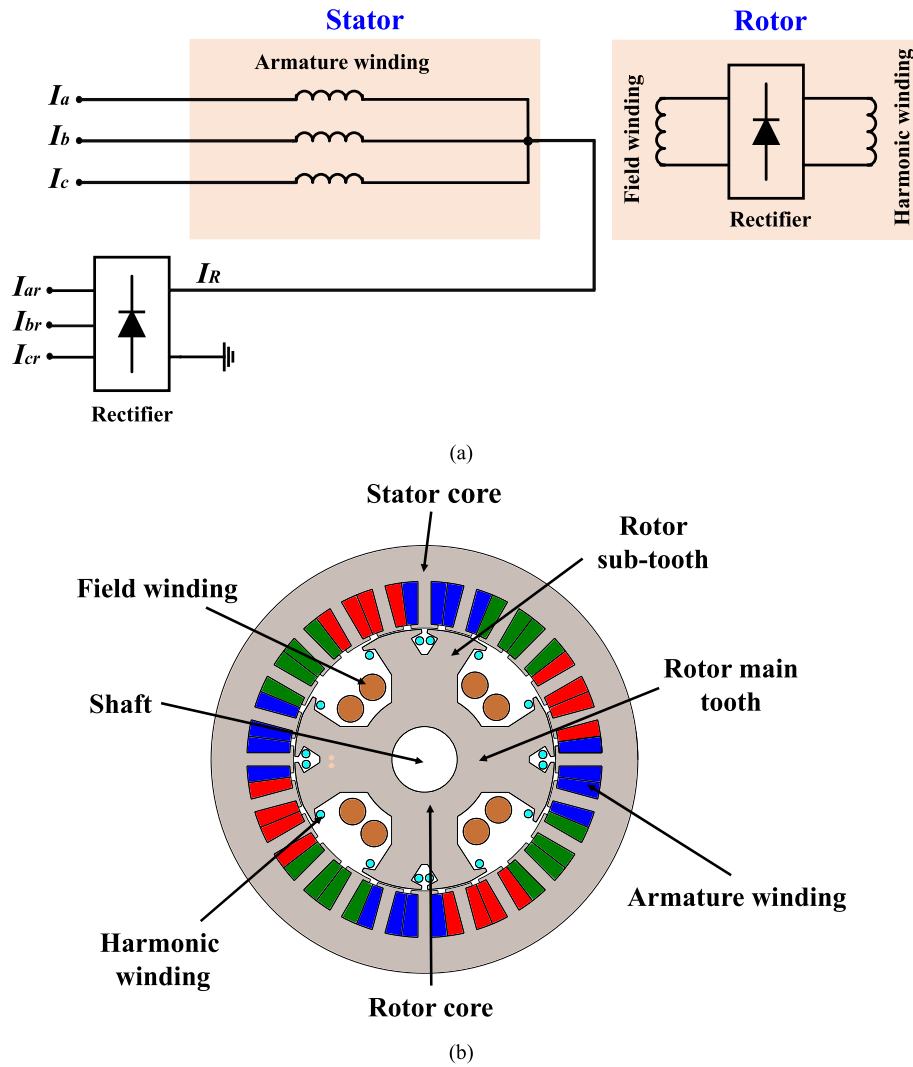
FIGURE 3. (a) Proposed simplified BL-WFSM topology, and (b) 2-D layout of the machine.
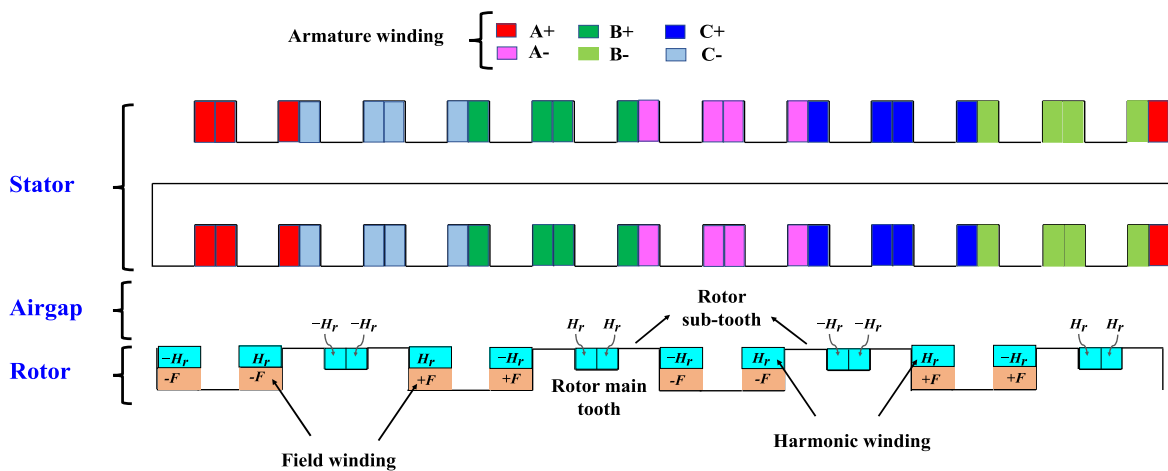
FIGURE 4. Machine winding configuration employed for the proposed BL-WFSM topology.

harmonic current that is equal to the output of the rectifier is generated for the armature winding through this arrangement. The assumption is also verified by plotting one phase of input and armature currents which shows that the same-phase input and armature currents which shows that the same-phase currents behave differently from each other after the injection of the rectifier output current. This behavior of the input and armature currents for one phase of the machine is shown in Fig. 6(b).
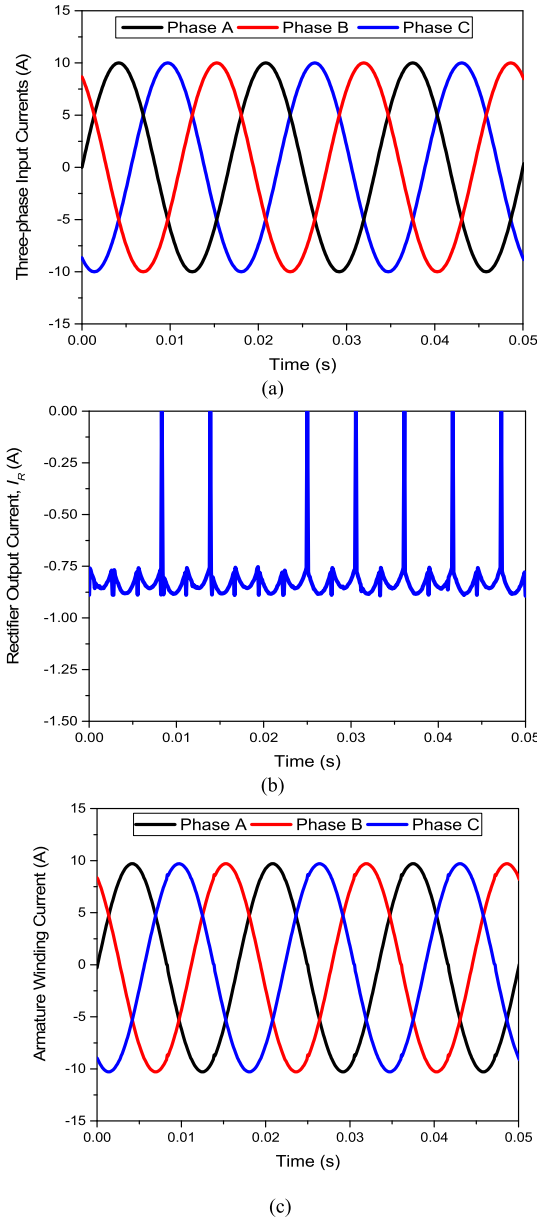
FIGURE 5. (a) Three-phase input; (b) rectifier output; and (c) armature winding currents.

As the armature winding is symmetrical, full-pitched, and concentrated, the MMF generated through each phase of the armature current i_a, i_b, and i_c can be calculated as below:

$$MMF_a = i_a N_{\varphi 1}(\sin\theta_s + \frac{1}{3}\sin 3\theta_s)$$

$$MMF_b = i_b N_{\varphi 1}\left\{\sin(\theta_s - \frac{2\pi}{3}) + \frac{1}{3}\sin 3\theta_s\right\}$$

$$MMF_c = i_c N_{\varphi 1}\left\{\sin(\theta_s + \frac{2\pi}{3}) + \frac{1}{3}\sin 3\theta_s\right\} \quad (1)$$

Here $N_{\varphi 1} = \frac{4}{\pi}\frac{N}{2}$

where N is the number of winding turns per phase, θ_s is the spatial electrical angle and ω is the electrical angular frequency.

The three-phase armature currents can be calculated as below:

$$i_a = I_1\sin(\omega t) + I_n$$

$$i_b = I_1\sin(\omega t - \frac{2\pi}{3}) + I_n$$

$$i_c = I_1\sin(\omega t + \frac{2\pi}{3}) + I_n \quad (2)$$

where I_1 is the fundamental current and I_n is the injected harmonic current in the armature winding.

By combining equation (1) and (2), and adding MMFs generated by three-phase armature currents, we have (3)–(6), as shown at the bottom of the next page.

From the above equation, it can be observed that the MMF generated by the armature winding is comprising of two components: the fundamental rotating MMF and the spatial fixed pulsating MMF caused by the injected harmonic current. These magnetic fields are generated at the same time in the airgap of the machine but are not coupled because of different operating frequencies [15]. When the rotor rotates at the same speed as that of the fundamental rotating field i.e., synchronous speed, the magnitude of the induced back-EMF in the harmonic and field windings of the machine will be zero. However, under such a condition the spatial fixed pulsating MMF generates back-EMF in the harmonic winding of the machine. If θ_0 is the angle of the initial position of harmonic winding, the spatial position of harmonic winding will be $\theta_s = \omega t + \theta_0$, as the rotor rotates at the synchronous speed. The flux of each winding pole, in this case, can be calculated as:

$$\psi_h = n_h P_g N_{\varphi 1}\left\{\frac{3}{2}I_1\cos(\omega t - \theta_s) + I_n\sin 3\theta_s\right\}$$

$$= n_h P_g N_{\varphi 1}\left\{\frac{3}{2}I_1\cos\theta_0 + I_n\sin(3\omega t + 3\theta_0)\right\} \quad (7)$$

where n_h is the harmonic winding number of turns, and P_g is the airgap permeance.

As the proposed simplified brushless WFSM topology is based on an uncontrolled three-phase customary rectifier, I_n will be equal to I_R which is pulsating DC output of the rectifier. The magnitude of the harmonic winding back-EMF is given by [15]:

$$EMF_h = 18 n_h P_g N_{\varphi 1}I_n\omega\cos(3\omega t + 3\theta_0) \quad (8)$$

where EMF_h is the induced back-EMF in the harmonic winding.

The induced harmonic voltages are rectified using a full-bridge rectifier, to generate the DC current for the rotor field winding and develop the rotor main field. This field generates torque as soon as it interacts with the main armature field, thereby achieving the proposed simplified brushless operation for the WFSM.

III. FINITE ELEMENT ANALYSIS

To validate the operation of the proposed simplified BL-WFSM topology and to obtain its electromechanical performance for the comparison with the existing three-phase
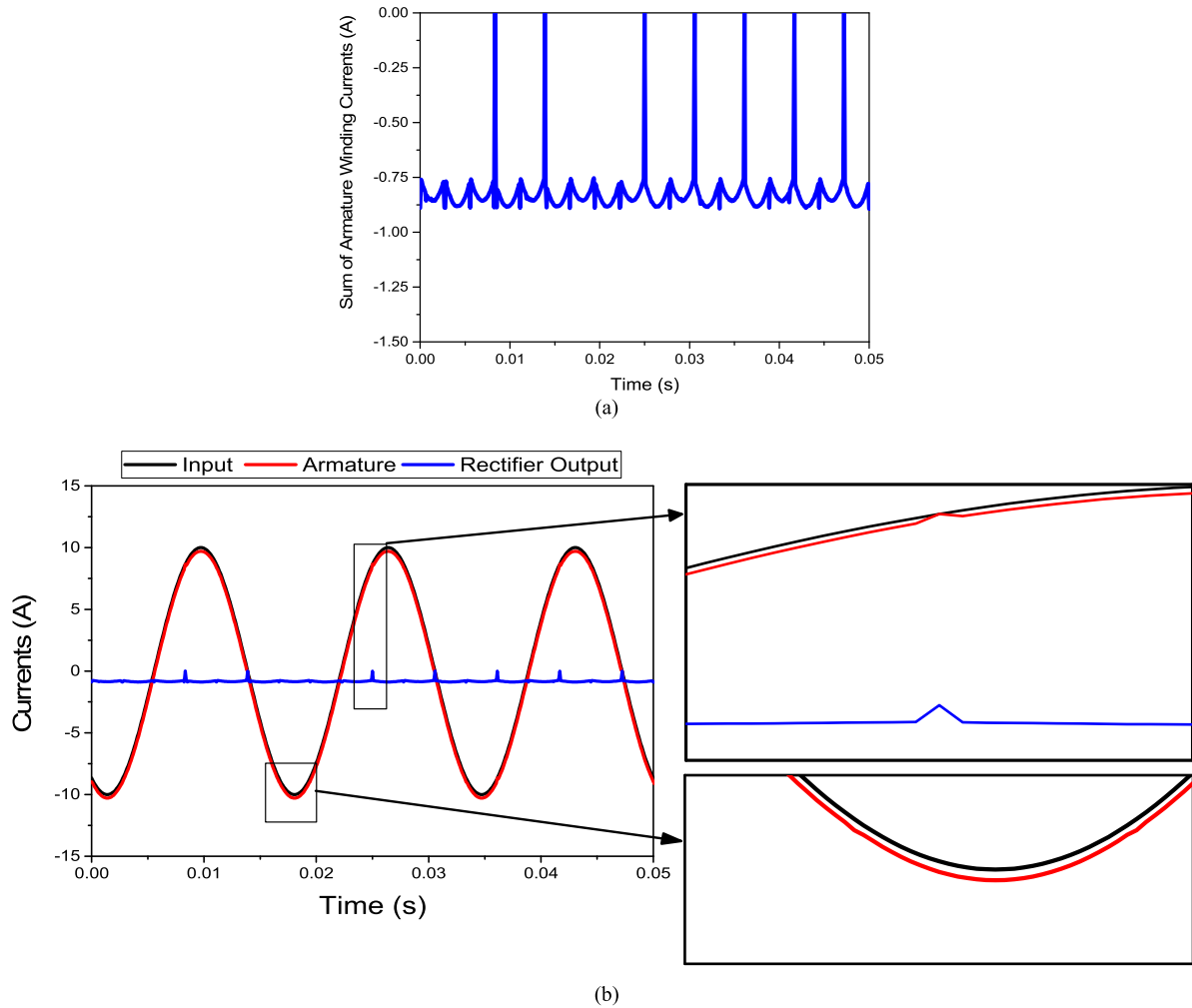
FIGURE 6. (a) Sum of three-phase armature winding currents and (b) input, armature, and rectifier output currents.

rectifier-based BL-WFSM topology, finite element analysis (FEA) was performed. Two 4-pole, 24-slot machine models with different armature winding configurations are used for this purpose. The specifications of the machine models are listed in Table 1. The winding pattern employed for the existing three-phase rectifier-based BL-WFSM topology is presented in Fig. 7. As shown in the figure, the rotor winding configuration of the proposed and existing BL-WFSM

$$MMF_{abc}(\theta_s, i) = MMF_a + MMF_b + MMF_c \tag{3}$$

$$= \begin{bmatrix} N_{\varphi 1} \left\{ \sin(\theta_s) + \frac{1}{3}\sin 3\theta_s \right\} \{I_1 \sin(\omega t) + I_n\} \\ + N_{\varphi 1} \left\{ \sin(\theta_s - \frac{2\pi}{3}) + \frac{1}{3}\sin 3\theta_s \right\} \left\{ I_1 \sin(\omega t - \frac{2\pi}{3}) + I_n \right\} \\ + N_{\varphi 1} \left\{ \sin(\theta_s + \frac{2\pi}{3}) + \frac{1}{3}\sin 3\theta_s \right\} \left\{ I_1 \sin(\omega t + \frac{2\pi}{3}) + I_n \right\} \end{bmatrix} \tag{4}$$

$$= N_{\varphi 1} \begin{bmatrix} I_1 \left\{ \begin{array}{l} \sin(\omega t)\sin(\theta_s) + \sin(\omega t - \frac{2\pi}{3})\sin(\theta_s - \frac{2\pi}{3}) \\ + \sin(\omega t + \frac{2\pi}{3})\sin(\theta_s + \frac{2\pi}{3}) \end{array} \right\} \\ + I_n \sin 3\theta_s \end{bmatrix} \tag{5}$$

$$= \frac{3}{2}I_1 N_{\varphi 1}\cos(\omega t - \theta_s) + I_n N_{\varphi 1}\sin 3\theta_s \tag{6}$$
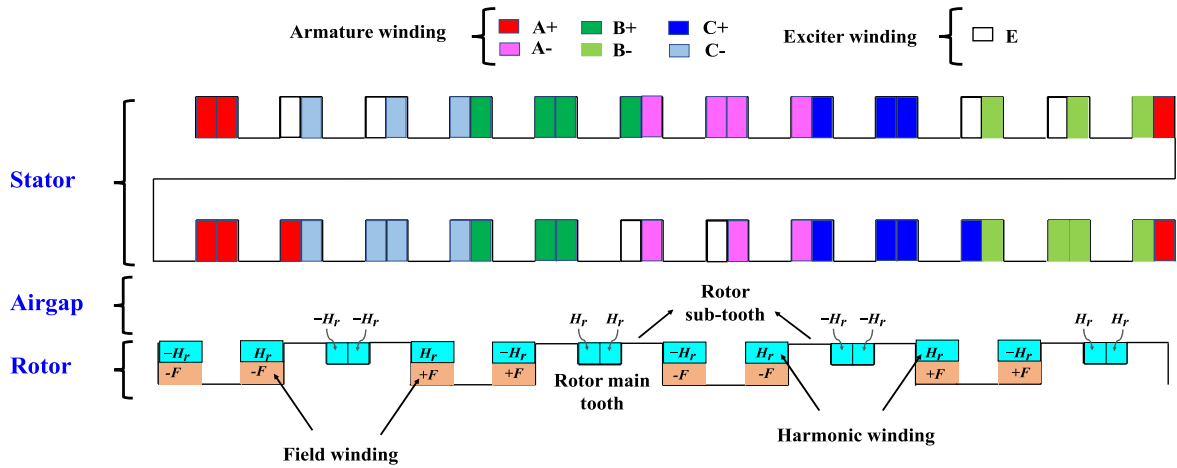
FIGURE 7. Machine winding configuration employed for the existing three-phase rectifier-based BL-WFSM topology.

(a)

(b)
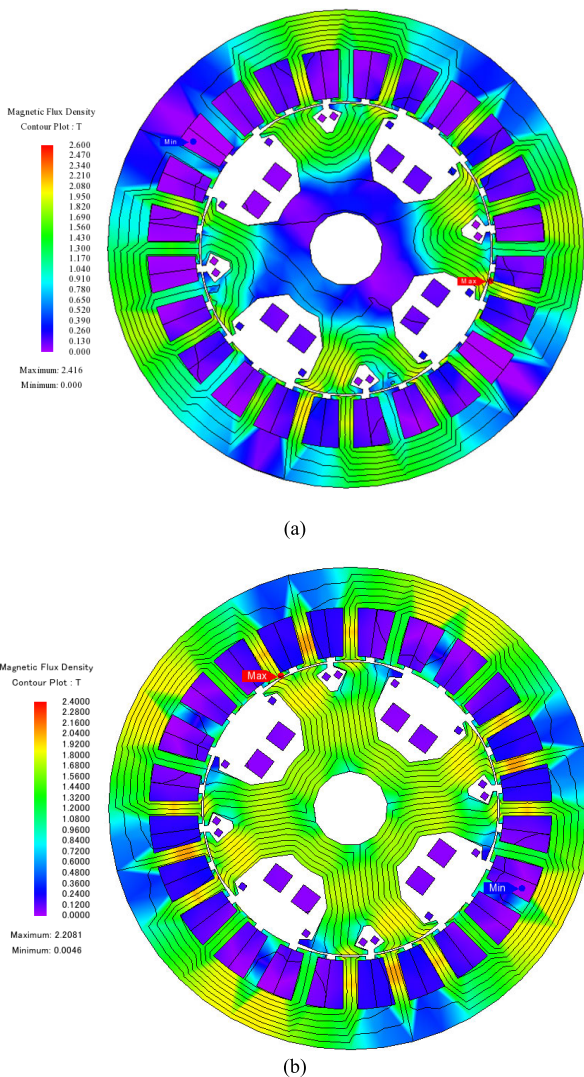
FIGURE 8. Flux density distribution plots for the (a) existing, and (b) proposed three-phase rectifier-based BL-WFSM topologies.

(a)

(b)

FIGURE 9. Flux linkages for the (a) existing, and (b) proposed three-phase rectifier-based BL-WFSM topologies.

topologies is the same, however, the armature winding of the proposed topology is altered by keeping two slots half-filled after a span of six slots. These half-filled slots are filled with the exciter winding in the existing three-phase rectifier-based BL-WFSM topology.

Both machines were operated at a constant speed of 1800 rpm and supplied with a current of 10 A (peak). A 4-pole, double-layered armature winding with a winding factor of 0.933 was employed for the investigated machine

TABLE 1. Machines Specifications.

Attribute	Existing BL-WFSM Topology	Proposed BL-WFSM Topology
Rated power	4 kW	4 kW
Rated speed	1800 rpm	1800 rpm
Frequency	60 Hz	60 Hz
Stator outer/inner diameter	130/80mm	130/80 mm
Air gap	0.5 mm	0.5 mm
Rotor diameter	79 mm	79 mm
Rotor main/sub-teeth	4/8	4/8
Harmonic/Field winding number of turns	25/250	25/250
Armature winding number of turns	100	100
Exciter winding number of turns	100	--
Stack length	90 mm	90 mm
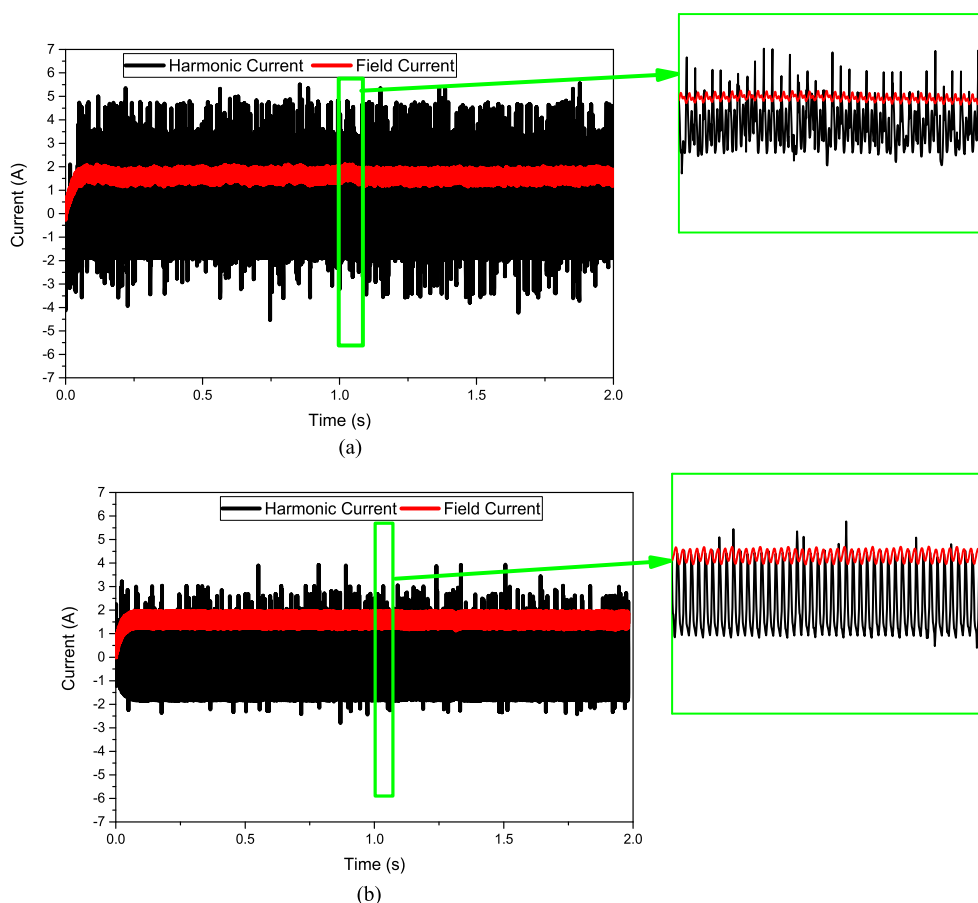
FIGURE 10. Induced harmonic and field currents for (a) existing, and (b) proposed three-phase rectifier-based BL-WFSM topologies.

models. The simulations were performed for 2s. The flux density distribution plots of the simulated existing and proposed three-phase rectifier-based BL-WFSM models are shown in Fig. 8(a) and (b), respectively. These plots show that the existing BL-WFSM operates under a saturation level of 2.6 T whereas the proposed machine topology operates below the saturation level of 2.4 T. The flux linkages for the existing

and proposed topologies are presented in Fig. 9(a) and (b), respectively. Fig. 10(a) and (b) illustrates the induced harmonic current in the harmonic winding and the rectified field current in the field winding of the existing and proposed machine models. These figures show that the average magnitude of the rectified field current for the existing BL-WFSM topology is around 1.56 A. However, the magnitude of the

(a)

(b)
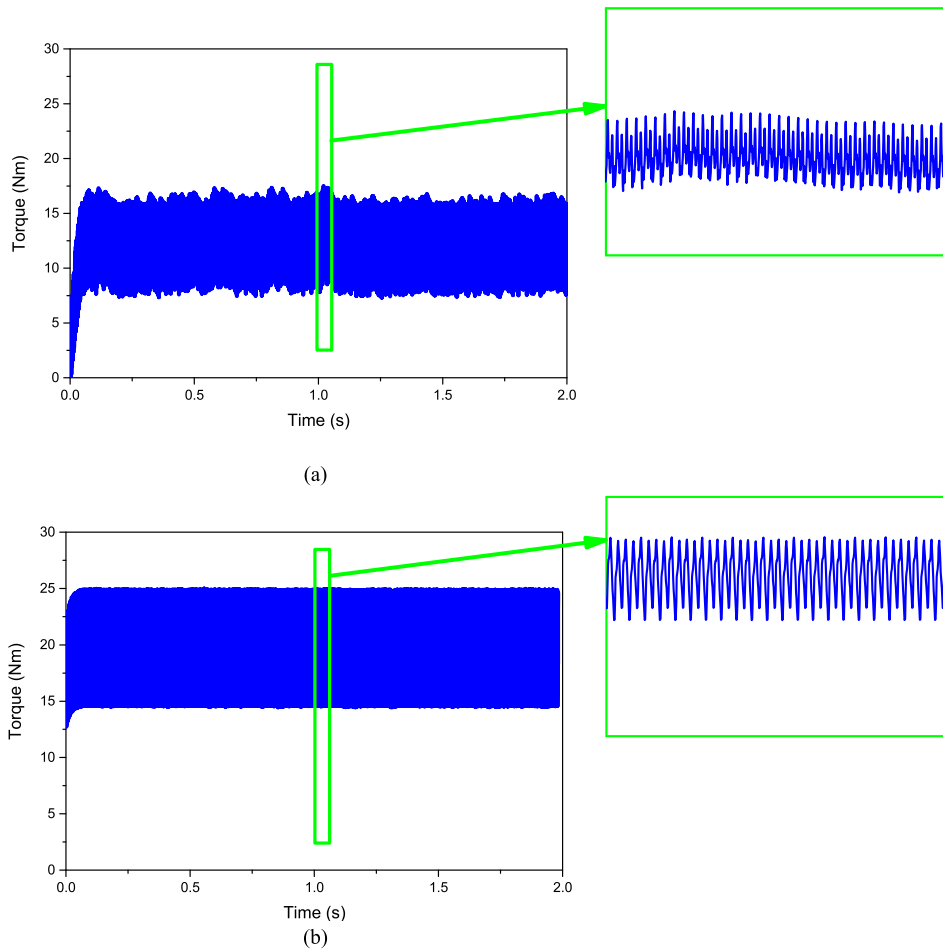
FIGURE 11. Output torque of the (a) existing, and (b) proposed BL-WFSM topologies.

TABLE 2. Comparative performance analysis.

Attribute	Existing BL-WFSM Topology	Proposed BL-WFSM Topology
Average output torque	11.29 Nm	20.15 Nm
Torque ripple	81.92%	51.30%
Efficiency	88.84%	96.83%

same current for the proposed topology is 1.58 A. The output torque of the existing and proposed machine models is shown in Fig. 11(a) and (b), respectively. The magnitude of the average torque of the existing three-phase rectifier-based BL-WFSM topology under steady-state is approximately 11.29 Nm with a torque ripple of 81.90%. On the other hand, the output torque of the proposed machine topology is 20.15 Nm with a ripple of 51.30%. The efficiency of the existing machine topology is calculated as 88.84% whereas the calculated efficiency of the proposed topology is 96.83%. These results indicate that the output torque of the proposed machine is around 78.47% higher than the existing three-phase rectifier-based BL-WFSM topology. In addition, the torque ripple for the proposed topology is decreased by around 30.6% when compared to the existing topology. Furthermore, the efficiency of the proposed topology is 7.99%

higher than the existing BL-WFSM topology. A comparative performance analysis between the existing and proposed three-phase rectifier-based BL-WFSM topologies is presented in Table. II.

To investigate the behavior of the existing and proposed machine models under no-load condition, simulations are carried out for one cycle using 1 A field current. The magnitude of the induced voltage for the existing machine topology under the no-load condition is around 270.48 V_{rms} as presented in Fig. 12(a). Fig. 12(b) shows the induced voltages of the proposed machine model under a no-load condition which is around 361.95 V_{rms}. The harmonic contents of the induced voltages for the existing and proposed topologies are shown in Fig. 12(c). The total harmonic distortion (THD) of the induced voltages for the existing and proposed BL-WFSM topologies during the no-load conditions is calculated as

TABLE 3. Comparative performance analysis under No-Load condition.

Attribute	Existing BL-WFSM Topology	Proposed BL-WFSM Topology
Induced Voltage	270.48 V_{rms}	361.95 V_{rms}
THD	24.53%	25.05%
Cogging torque	0.61 Nm	0.59 Nm
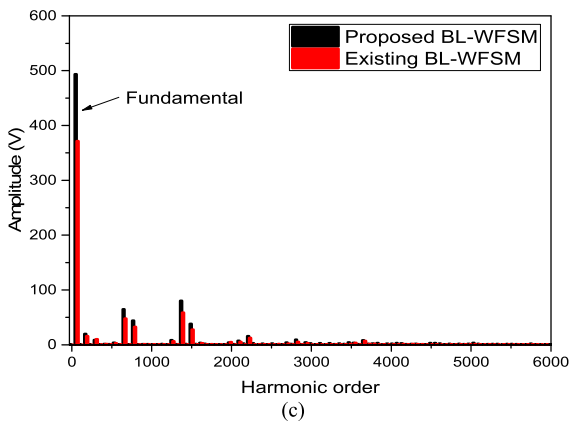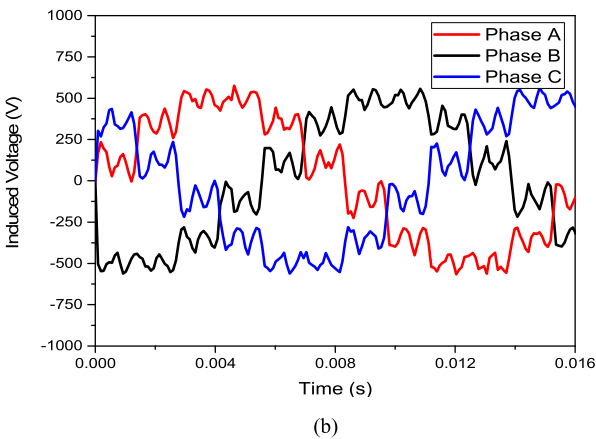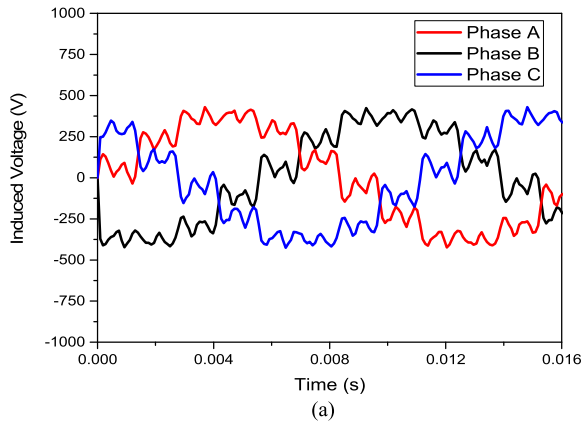
FIGURE 12. Induced voltages under no-load condition for (a) existing, and (b) proposed BL-WFSM topologies, and (c) harmonic contents of the induced voltages.

24.53%, and 25.05%, respectively using equation (9):

$$THD = \frac{\sqrt{V_2^2 + V_3^2 + V_4^2 + V_5^2 + \ldots\ldots + V_n^2}}{V_1} \quad (9)$$
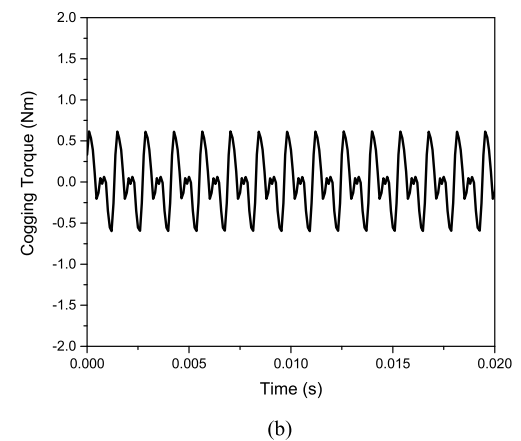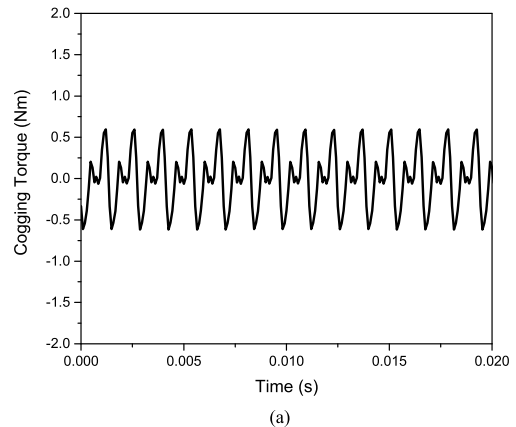
FIGURE 13. Cogging torque for the (a) existing, and (b) proposed three-phase rectifier-based BL-WFSM topologies.

where V_1 is the fundamental component and V_n is the *nth* harmonic component of the induced voltage.

The magnitude of the cogging torque for the existing and proposed WFSM topologies is 0.61 Nm and 0.59 Nm as shown in Fig. 13(a) and (b), respectively. This comparative performance analysis under a no-load condition is provided in Table. III.

IV. CONCLUSION

A simplified brushless WFSM topology was proposed in this paper. The proposed topology was based on a rectifier; its output was injected into the common point of the star-connected armature winding. This arrangement generated a harmonic MMF that is used to induce a harmonic current in the harmonic winding of the rotor. The induced harmonic current was rectified to generate a DC current for the rotor field excitation and achieves brushless operation. FEA was conducted

for a 4-pole, 24-slot machine model to realize the idea and obtain the output torque of the machine. The average output torque of the machine was found to be 20.15 Nm with a torque ripple of 51.30%.

The proposed topology was compared with the existing three-phase rectifier-based BL-WFSM topology which showed that the output torque is increased up to 78.47%, torque ripple is decreased to 30.6% and efficiency is increased to 7.99% for the proposed topology when compared to the existing BL-WFSM topology.

The proposed BL–WFSM topology was based on a customary uncontrolled three-phase rectifier that did not require any complex hardware and control mechanisms. Thus, it proved to be the simplest and most cost-effective brushless topology compared to the other brushless topologies reported in the literature.

REFERENCES

[1] S. S. H. Bukhari, G. J. Sirewal, F. A. Chachar, and J.-S. Ro, "Brushless field excitation scheme for wound field synchronous machines," *Appl. Sci.*, vol. 10, no. 17, p. 5866, Aug. 2020.

[2] S. S. H. Bukhari, G. J. Sirewal, S. Madanzadeh, and J.-S. Ro, "Cost-effective single-inverter-controlled brushless technique for wound rotor synchronous machines," *IEEE Access*, vol. 8, pp. 204804–204815, 2020.

[3] M. Ayub, S. S. H. Bukhari, G. Jawad, and B.-I. Kwon, "Reluctance torque utilization to improve the starting and average torques of a brushless wound field synchronous machine," in *Proc. 19th Int. Symp. Appl. Electromagn. Mech. (ISEM)*, Sep. 2019.

[4] F. Yao, D. Sun, L. Sun, and T. A. Lipo, "Dual third-harmonic-current excitation principle of a brushless synchronous machine based on double three-phase armature windings," in *Proc. 22nd Int. Conf. Electr. Mach. Syst. (ICEMS)*, Harbin, China, Aug. 2019, pp. 1–4.

[5] Q. Ali, S. S. H. Bukhari, and S. Atiq, "Variable-speed, sub-harmonically excited BL-WRSM avoiding unbalanced radial force," *Electr. Eng.*, vol. 101, no. 1, pp. 251–257, Apr. 2019.

[6] M. Ayub, S. Bukhari, G. Sirewal, and B. Kwon, "Brushless wound rotor synchronous machine with third harmonic field excitation using single inverter," in *Proc. IEEE Int. Magn. Conf. (INTERMAG)*, Apr. 2018.

[7] K. Inoue, H. Yamashita, E. Nakamae, and T. Fujikawa, "A brushless self-exciting three-phase synchronous generator utilizing the 5th-space harmonic component of magneto motive force through armature currents," *IEEE Trans. Energy Convers.*, vol. 7, no. 3, pp. 517–524, Sep. 1992.

[8] G. Jawad, Q. Ali, T. A. Lipo, and B.-I. Kwon, "Novel brushless wound rotor synchronous machine with zero-sequence third-harmonic field excitation," *IEEE Trans. Magn.*, vol. 52, no. 7, pp. 1–4, Jul. 2016.

[9] F. Yao, Q. An, L. Sun, and T. A. Lipo, "Performance investigation of a brushless synchronous machine with additional harmonic field windings," *IEEE Trans. Ind. Electron.*, vol. 63, no. 11, pp. 6756–6766, Nov. 2016.

[10] Q. An, X. Gao, F. Yao, L. Sun, and T. Lipo, "The structure optimization of novel harmonic current excited brushless synchronous machines based on open winding pattern," in *Proc. IEEE Energy Convers. Congr. Expo. (ECCE)*, Pittsburgh, PA, USA, Sep. 2014, pp. 1754–1761.

[11] M. Ayub, G. Jawad, S. S. H. Bukhari, and B.-I. Kwon, "Brushless wound rotor synchronous machine with third-harmonic field excitation," *Electr. Eng.*, vol. 102, no. 1, pp. 259–265, 2020.

[12] S. S. H. Bukhari, G. J. Sirewal, F. A. Chachar, and J.-S. Ro, "Dual-inverter-controlled brushless operation of wound rotor synchronous machines based on an open-winding pattern," *Energies*, vol. 13, no. 9, p. 2205, May 2020.

[13] M. Ayub, S. S. H. Bukhari, G. Jawad, and B.-I. Kwon, "Brushless wound field synchronous machine with third-harmonic field excitation using a single inverter," *Electr. Eng.*, vol. 101, no. 1, pp. 165–173, Apr. 2019.

[14] S. S. H. Bukhari, G. J. Sirewal, M. Ayub, and J.-S. Ro, "A new small-scale self-excited wound rotor synchronous motor topology," *IEEE Trans. Magn.*, early access, Jul. 15, 2020, doi: 10.1109/TMAG.2020.3009372.

[15] L. Sun, X. Gao, F. Yao, Q. An, and T. Lipo, "A new type of harmonic current excited brushless synchronous machine based on an open winding pattern," in *Proc. IEEE Energy Convers. Congr. Expo. (ECCE)*, Pittsburgh, PA, USA, Sep. 2014, pp. 2366–2373.

SYED SABIR HUSSAIN BUKHARI (Member, IEEE) received the B.E. degree in electrical engineering from the Mehran University of Engineering and Technology, Jamshoro, Pakistan, in 2009, and the Ph.D. degree from the Department of Electronic Systems Engineering, Hanyang University, South Korea, in 2017. In December 2016, he joined Sukkur IBA University, as an Assistant Professor. He is currently working as a Research Professor with Chung-Ang University, Seoul, South Korea, under Korean Research Fellowship (KRF) program. His main research interests include electric machine design, power quality, and drive controls.

HAMZA AHMAD (Graduate Student Member, IEEE) received the B.S. degree in electrical engineering from the Pakistan Institute of Engineering and Applied Sciences (PIEAS), Pakistan, in 2018. He is currently pursuing the M.S. degree with Chung-Ang University, Seoul, South Korea, as a Graduate Research Assistant. His research interests include the design and optimization of electrical machines and applications of electromagnetic smart materials.

GHULAM JAWAD SIREWAL was born in Tando Allahyar, Pakistan, in 1988. He received the B.E. degree in electrical engineering and the P.G.D. degree in electrical power engineering from the Mehran University of Engineering and Technology, Jamshoro, Pakistan, in 2011 and 2012, respectively, and the Ph.D. degree from the Department of Electrical and Electronic Engineering, Hanyang University, Ansan, South Korea, in 2020. He is currently an Assistant Professor with the Department of Electrical Engineering Technology, The Benazir Bhutto Shaheed University of Technology and Skill Development, Khairpur Mir's, Pakistan. His research interest includes electric machine design and control.

JONG-SUK RO received the B.S. degree in mechanical engineering from Hanyang University, Seoul, South Korea, in 2001, and the Ph.D. degree in electrical engineering from Seoul National University (SNU), Seoul, in 2008.

From 2008 to 2012, he conducted research at the Research and Development Center, Samsung Electronics, as a Senior Engineer. From 2012 to 2013, he was with the Brain Korea 21 Information Technology, SNU, as a Postdoctoral Fellow. He conducted research at the Electrical Energy Conversion System Research Division, Korea Electrical Engineering and Science Research Institute, as a Researcher, in 2013. From 2013 to 2016, he worked with the Brain Korea 21 Plus, SNU, as a BK Assistant Professor. In 2014, he was with the University of BATH, Bath, U.K. He is currently an Associate Professor with the School of Electrical and Electronics Engineering, Chung-Ang University, Seoul. His research interests include the analysis and optimal design of next-generation electrical machines using smart materials, such as electromagnet, piezoelectric, magnetic shape memory alloy, and so on.

● ● ●